Syntheses, Structures and Photocatalytic Degradation Properties of Two Copper(II) Coordination Polymers with Flexible Bis(imidazole) Ligand①

ZHANG Yong[a] QIN Hong-Ni[a] LI Bao-Long[b②] WU Bing[b]

[a] (*China Suzhou Industrial Park Institute of Services Outsourcing, Suzhou* 215123, *China*)

[b] (*State and Local Joint Engineering Laboratory for Functional Polymeric Materials, College of Chemistry, Chemical Engineering and Materials Science, Soochow University, Suzhou* 215123, *China*)

ABSTRACT Two copper(II) coordination polymers $\{[Cu(bib)(nip)]\cdot 1.5H_2O\}_n$ (**1**) and $[Cu_2(bib)(glu)_2]_n$ (**2**) (bib = 1,4-bis(2-methyl-imidazol-1-yl)butane, H_2nip = 5-nitroisophthalic acid, H_2glu = glutaric acid) were synthesized by the hydrothermal method and characterized by single-crystal X-ray diffraction, elemental analyses, IR and solid-state diffuse-reflection spectra. **1** forms a 2*D* network with the point symbol of $(4^4\ 6^2)$ and $2D \rightarrow 2D$ polythreaded network. **2** constructs the 6-connected 3*D* network based on the $[Cu_2(COO)_2]$ dimer with the point symbol of $(4^4\ 6^{10}\ 8)$. The energy band gaps (E_g) of **1** and **2** were 2.453 and 2.162 eV, respectively. **1** and **2** present high photocatalytic activity for the degradation of methylene blue under visible light irradiation.

Keywords: coordination polymer, structure, 3D network, photocatalysis,1,4-bis(2-methyl-imidazol-1-yl)butane; DOI: 10.14102/j.cnki.0254–5861.2011–2989

1 INTRODUCTION

Water pollution issue is an important environmental problem with the modern industrial development and the population growth recently[1]. The organic dyes from textiles and dye industries are one of the kinds of important contaminations which result into water pollution and environmental problem[2]. The conventional biological treatment methods and physical methods, such as adsorption and coagulation, are the main techniques to remove organic dyes from the wastewater[3]. However, these conventional methods do not eliminate dyes and may produce secondary pollutants. Therefore, the development of new methods to remove organic dyes from wastewater with high efficiency and low cost is very helpful for the wastewater treatment and environment protection.

The inorganic semiconductors such as TiO_2, ZnO, CuO, Ag_2O, ZnS and CdS have been developed for photocatalytic degradation of organic pollutants under UV light irradiation[4-7]. Since MOF-5 was used as photocatalyst for the degradation of phenol[8], the MOF photocatalysts have been exploited by inorganic and materials scientists for the photocatalytic degradation of organic dyes[9-12]. However, there is still a great challenge to obtain new MOF photocatalysts with high efficiency and low cost under visible light irradiation.

Coordination polymers have gained great interest due to their intriguing topologies and potential applications as functional materials like gas separation and storage[13], nonlinear optics[14], magnetism[15], luminescence[16, 17], chemical sensors[18, 19] and photocatalysis[20] in recent two decades. The organic ligands and metal central atoms play the key role in the assembly of coordination polymers[21-23].

The combination ligands systems based on N-donor ligands (such as imidazole and triazole ligands) and O-donor ligands (multicarboxylate ligands) and metal central cations can construct coordination polymers with various topologies and multifunctional properties[24, 25]. The flexible bis(imidazole) ligand 1,4-bis(2-methyl-imidazol-1-yl)butane is a good N-donor ligand for the assembly of coordination polymers[26, 27]. In the present work, the bispodal N-donor imidazole ligand 1,4-bis(2-methyl-imidazol-1-yl)butane and biscarboxylate

Received 22 September 2020; accepted 25 November 2020 (**CCDC 2001545** for **1** and **2001546** for **2**)

① This project was supported by the Natural Science Foundation of Jiangsu Province (No. BK20161212), the Priority Academic Program Development of Jiangsu Higher Education Institutions, and the project of scientific and technological infrastructure of Suzhou (SZS201905)

② Corresponding author. Li Bao-Long. E-mail: libaolong@suda.edu.cn

ligand system was selected for the synthesis of new coordination polymers. Therefore, two copper(II) coordination polymers $\{[Cu(bib)(nip)]\cdot 1.5H_2O\}_n$ (**1**) and $[Cu_2(bib)(glu)_2]_n$ (**2**) were synthesized by the hydrothermal method (bib = 1,4-bis(2-methyl-imidazol-1-yl)butane, H_2nip = 5-nitroisophthalic acid, H_2glu = glutaric acid). The syntheses, crystal structure, and photocatalytic properties were studied.

2 EXPERIMENTAL

2. 1 Materials and general methods

All other reagents were of analytical grade and used without purification. Elemental analyses for C, N, and H were performed on a Perkin-Elmer 240C analyzer. UV-vis diffuse-reflection spectra of the solid samples were collected with a Cary 500 spectrophotometer. IR spectra were obtained for KBr pellets on a Nicolet 170SX FT-IR spectrophotometer from 4000 to 400 cm^{-1}.

2. 2 Synthesis of $\{[Cu(bib)(nip)]\cdot 1.5H_2O\}_n$ (1)

The aqueous solution (8 mL) of H_2nip (1.00 mmol) and bib (1.00 mmol) was adjusted to pH 6 with 1.0 M NaOH solution. Then the aqueous solution (5 mL) of $Cu(NO_3)_2\cdot 2.5H_2O$ (1.50 mmol) was added and stirred for ten minutes. The above solution was sealed in a Teflon-lined stainless-steel vessel (25 mL) and heated to 120 ℃ for 72 h. The blue crystals **1** were obtained (Yield: 0.252 g, 48.6% based on bib). Anal. Calcd. for $C_{20}H_{24}CuN_5O_{7.50}$ (**1**): C, 46.38; H, 4.67; N, 13.52%. Found: C, 46.19; H, 4.64; N, 13.45%. IR data (cm^{-1}): 3370m, 3223m, 1623s, 1566m, 1534m, 1453m, 1424m, 1364s, 1282w, 1152w, 1122w, 1101w, 1015w, 903w, 787m, 737s, 680w.

2. 3 Synthesis of $[Cu_2(bib)(glu)_2]_n$ (2)

The aqueous solution (10 mL) of H_2glu (1.00 mmol) and bib (0.50 mmol) was adjusted to pH 6 with 1.0 M NaOH solution. Then the aqueous solution (5 mL) of $Cu(NO_3)_2\cdot 2.5H_2O$ (1.20 mmol) was added and stirred for ten minutes. The above solution was sealed in a Teflon-lined stainless-steel vessel (25 mL) and heated to 110 ℃ for 48 h. Block blue crystals **2** were obtained (Yield: 0.159 g, 52.5% based on bib). Anal. Calcd. for $C_{22}H_{30}Cu_2N_4O_8$ (**2**): C, 43.63; H, 4.99; N, 10.04%. Found: C, 43.54; H, 4.94; N, 9.98%. IR data (cm^{-1}): 1616s, 1534m, 1449m, 1412s, 1314w, 1280m, 1163w, 1070m, 805m, 760m, 670s, 651m, 632m.

2. 4 Photocatalytic experiment

The experiment was performed on a PCR-I multipurpose photoreactor equipped a CEL-HXF300 Xe lamp with UV cut-off filter (providing visible light with λ > 400 nm) (Beijing China Education Au-Light Company Limited, China). The crystalline samples of **1** or **2** (20 mg) and 0.50 mL 30% H_2O_2 were added into the methylene blue (MB) (10 mg/L) solution (100 mL). The suspension solutions were stirred in the dark room for 30 min. Then, the suspension solutions were stirred continuously under visible light irradiation. At a given interval, the aliquots of the reaction solutions were taken and analyzed with a UV-vis spectrophotometer at 664 nm.

2. 5 Structure determination

X-ray crystallography suitable single crystals **1** and **2** were carefully selected under an optical microscope and glued to thin glass fibers. The diffraction data were collected on a Rigaku Mercury CCD diffractometer at 293(2) K with graphite-monochromated Mo-$K\alpha$ radiation (λ = 0.71073 Å). The structures were solved by direct methods using SHELXS-2016[28] and refined with full-matrix least-squares technique using SHELXL-2016[29]. The final R = 0.0851, wR = 0.2127 ($w = 1/[\sigma^2(F_o^2) + (0.1133P)^2 + 1.9302P]$, where $P = (F_o^2 + 2F_c^2)/3$), $(\Delta/\sigma)_{max}$ = 0.000, S = 1.085, $(\Delta\rho)_{max}$ = 0.699 and $(\Delta\rho)_{min}$ = –0.531 e·Å^3 for **1**. The final R = 0.0766, wR = 0.1430 ($w = 1/[\sigma^2(F_o^2) + (0.00500P)^2 + 8.5268P]$, where $P = (F_o^2 + 2F_c^2)/3$), $(\Delta/\sigma)_{max}$ = 0.000, S = 1.133, $(\Delta\rho)_{max}$ = 0.367 and $(\Delta\rho)_{min}$ = –0.357 e·Å^3 for **2**.

3 RESULTS AND DISCUSSION

3. 1 Crystal structure of 1

Single-crystal X-ray diffraction analysis showed that **1** belongs to triclinic space group of $P\bar{1}$. The asymmetric unit of **1** consists of one Cu(II) cation (Cu(1), one bib, one nip^{2-} anion ligand, and one and half lattice water. Each Cu(II) cation is coordinated by three carboxylate oxygen atoms (O(1), O(3B), O(4B)) from two nip^{2-} ligands and two imidazole nitrogen atoms (N(2), N(4A)) from two bib ligands in the distorted square-pyramidal geometry (Fig. 1a). Two largest coordination angles are 166.3(2)° for N(2)–Cu(1)–N(4A) and 160.2(2)° for O(1)–Cu(1)–O(3B) (Table 1). The trigonal distort from square-pyramidal geometry index τ is 0.102, indicating its square-pyramidal geometry. Each bib shows the gauche-anti-gauche conformation and behaves as a 2-nodal ligand with its two imidazole nitrogen atoms (N(2) and N(4)) and joins two Cu(II) cations with the Cu··Cu distance of 12.702(6) Å. One carboxylate group (O(1)O(2) of nip^{2-} exhibits a monodentate coordination mode with O1 coordination atom. Other carboxylate group (O(3)O(4)) of nip^{2-} presents a chelating coordination mode with O(3) and

O(4) coordination atoms. Each nip^{2-} also behaves as a 2-nodal ligand and connects two Cu(II) cations with the Cu ··Cu distance of 10.154(6) Å.

Table 1. Selected Bond Lengths (Å) and Bond Angles (°) for 1

Bond	Dist.	Bond	Dist.	Bond	Dist.
Cu(1)–N(2)	1.976(5)	Cu(1)–N(4)^{a}	2.059(6)	Cu(1)–O(1)	1.956(4)
Cu(1)–O(3)^{b}	2.044(4)	Cu(1)–O(4)^{b}	2.354(5)		
Angle	(°)	Angle	(°)	Angle	(°)
N(2)–Cu(1)–N(4)^{a}	166.3(2)	N(2)–Cu(1)–O(1)	95.0(2)	N(2)–Cu(1)–O(3)^{b}	160.2(2)
N(2)–Cu(1)–O(4)^{b}	93.7(2)	N(4)^{a}–Cu(1)–O(1)	89.1(2)	N(4)^{a}–Cu(1)–O(3)^{b}	92.1(2)
N(4)^{a}–Cu(1)–O(4)^{b}	98.5(2)	O(1)–Cu(1)–O(3)^{b}	160.2(2)	O(1)–Cu(1)–O(4)^{b}	100.58(19)
O(3)^{b}–Cu(1)–O(4)^{b}	59.71(17)				

Symmetry transformation: a: *x*, *y*, *z*–1; b: *x*+1, *y*, *z* for **1**

Table 2. Selected Bond Lengths (Å) and Bond Angles (°) for 2

Bond	Dist.	Bond	Dist.	Bond	Dist.
Cu(1)–O(1)	1.981(4)	Cu(1)–O(2)^{a}	1.974(5)	Cu(1)–O(4)^{b}	1.983(4)
Cu(1)–O(3)^{b}	1.988(4)	Cu(1)–N(2)	2.142(5)		
Angle	(°)	Angle	(°)	Angle	(°)
O(1)–Cu(1)–O(2)^{a}	167.05(19)	O(1)–Cu(1)–O(4)^{b}	90.16(19)	O(1)–Cu(1)–O(3)^{c}	88.4(2)
O(1)–Cu(1)–N(2)	96.2(2)	O(2)^{a}–Cu(1)–O(4)^{b}	88.7(2)	O(2)^{a}–Cu(1)–O(3)^{b}	89.7(2)
O(2)^{a}–Cu(1)–N(2)	96.73(19)	O(4)^{b}–Cu(1)–O(3)^{c}	166.6(2)	O(4)^{b}–Cu(1)–N(2)	97.1(2)
O(3)^{c}–Cu(1)–N(2)	96.3(2)				

Symmetry transformation: a: –*x*+1/2, –*y*+1/2, –*z*+2; b: –*x*+1/2, *y*+2, –*z*+3/2, c: *x*, –*y*, *z*+1/2 for **2**

Each Cu(II) cation is coordinated with two bib and two nip^{2-} ligands and presents a 2*D* network (Fig. 1b) with the point symbol of $(4^4 6^2)$. Two adjacent 2*D* networks polythreaded each other with their nitro groups and show a 2*D* → 2*D* polythreaded network (Fig. 1c).

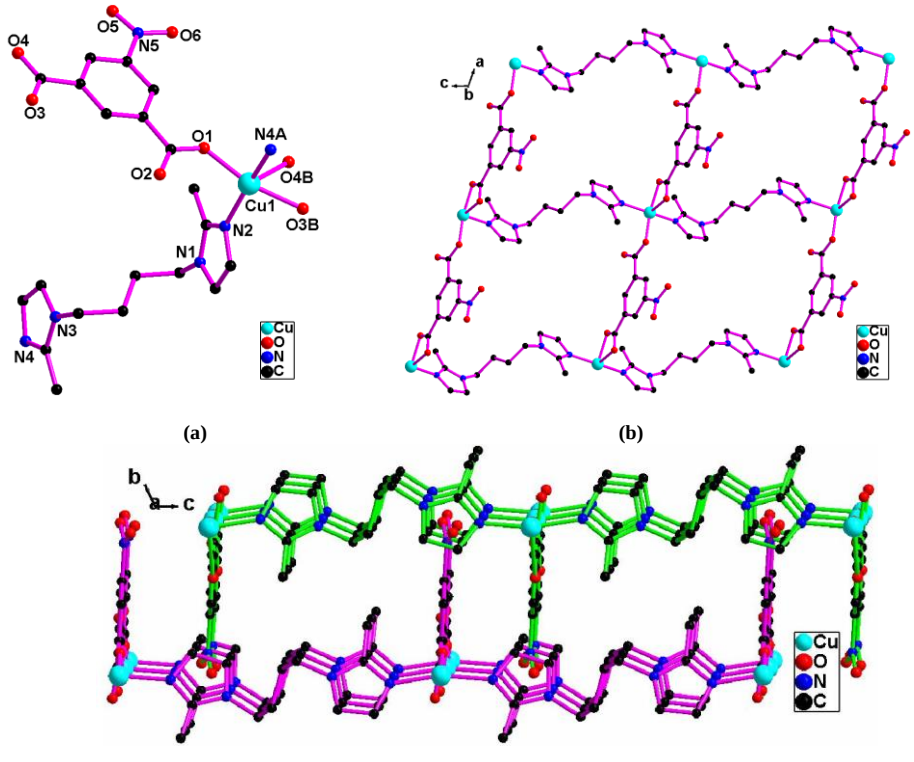

Fig. 1. (a) Coordination environment of the copper(II) cation in 1. Symmetry cods: A *x*, *y*, *z*–1; B *x*+1, *y*, *z*. (b) Two-dimensional network in 1. (c) 2*D* → 2*D* polythreaded network in 1

3. 2 Crystal structure of 2

2 crystallizes in the monoclinic space group of *C*2/*c*. The asymmetric unit of **2** consists of one copper(II) cation (Cu1), half bib and one glu^{2-} ligand. The Cu(1) cation is coordinated with four carboxylate oxygen atoms (O(1), O(2A), O(3C), O(4B)) from four glu^{2-} ligands in the square plane and one imidazole nitrogen atom (N(2)) from one bib ligand in the apex position with the square-pyramidal geometry (Fig. 2a). Two largest coordination angles are 167.05(19)° for O(1)–Cu(1)– O(2A) and 166.6(2)° for O(4B)–Cu(1)–O(3C) (Table 2). The trigonal distortion from square-pyramidal geometry index τ is 0.0075, indicating its square-pyramidal geometry. Two carboxylate groups (O(1)O(2) and O(3)O(4)) of one glu^{2-} ligand both perform the bidentate coordination modes and coordinate two copper(II) cations with the Cu ··Cu distance of 2.6795(5) Å. One glu^{2-} ligand acts as a tetra-dentate coordination mode and connects four copper(II) cations (Fig. 2b). The copper(II) cations are joined by glu^{2-} ligands and produce a $[Cu_2(glu)_2]_n$ two-dimensional network (Fig. 2c).

Each bib exhibits the *anti-anti-anti* conformation and bridges two copper(II) cations with the Cu ··Cu distance of 12.112(2) Å. The $[Cu_2(glu)_2]_n$ two-dimensional networks are connected by bib ligands and form a three-dimensional network (Fig. 2d). According to the topological analysis[30], the $[Cu_2(COO)_2]$ dimer can be simplified as a 6-connected node. The bib and glu^{2-} ligands are 2-connected nodes. The point symbol of 3*D* network of **2** is (4^4 6^{10} 8).

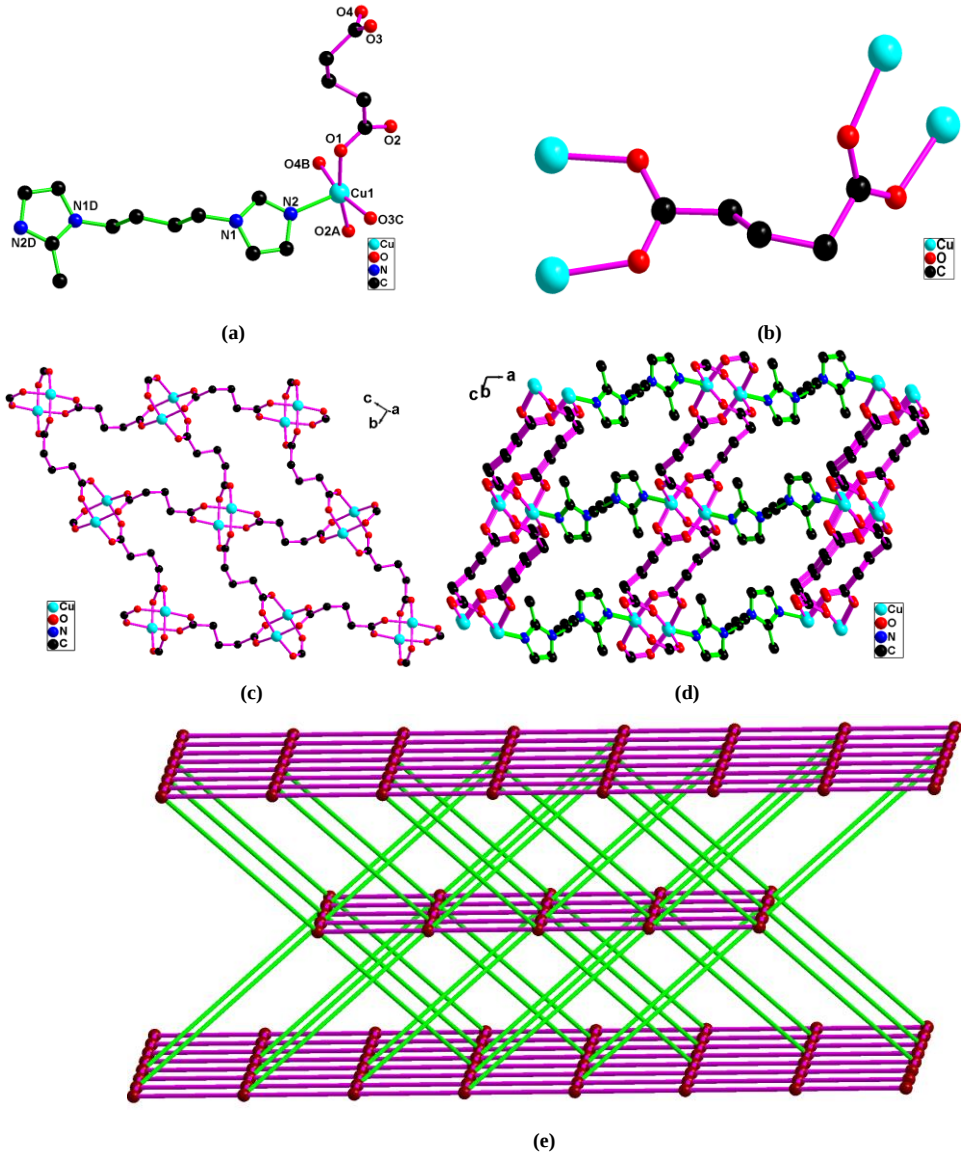

Fig. 2. (a) Coordination environment of the copper(II) cation in 2. Symmetry cods: A: –*x*+1/2, –*y*+1/2, –*z*+2; B: –*x*+1/2, *y*+1/2, –*z*+3/2; C: *x*, –*y*, *z*+1/2; D: –*x*+1, –*y*+2, –*z*+2. (b) Coordination mode of glu^{2-} ligand. (c) Two-dimensional network $[Cu_2(glu)_2]_n$. (d) Three-dimensional network in 2. (e) 6-Connected 3*D* network in 2. The black red balls show 6-connected $[Cu_2(COO)_2]$ dimer. Pink and bright green sticks exhibit glu and bib ligands, respectively

3. 3 Solid-state diffuse-reflection spectra and catalytic activity for the degradation of methylene blue

Solid-state diffuse-reflection spectra of crystalline solids **1** and **2** were investigated at room temperature. The absorption data were obtained according to the Kubelka-Munk function using the reflection data. The energy band gaps (E_g) of **1** and **2** were 2.453 and 2.162 eV, respectively, according to the extrapolation of the linear portion of the absorption edges (Fig. 3). The low E_g values exhibit that **1** and **2** should have semiconductor nature and photocatalytic activity.

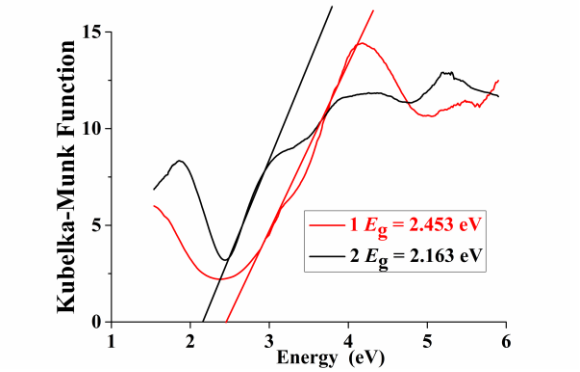

Fig. 3. Solid-state optical diffuse-reflection spectra of crystalline solids 1 and 2

The photocatalytic degradation of methylene blue (MB) using **1** and **2** as catalysts was presented in Figs. 4, 5 and 6. The degradation efficiency was merely 17.7% in the blank experiment (only H_2O_2) after 105 min visible light irradiation. The degradation efficiencies reached 91.5% and 95.5% using catalysts **1** and **2**, respectively, at the same experimental conditions and time (105 min). The photocatalytic experimental result exhibited that **1** and **2** are good photocatalysts for the degradation of MB.

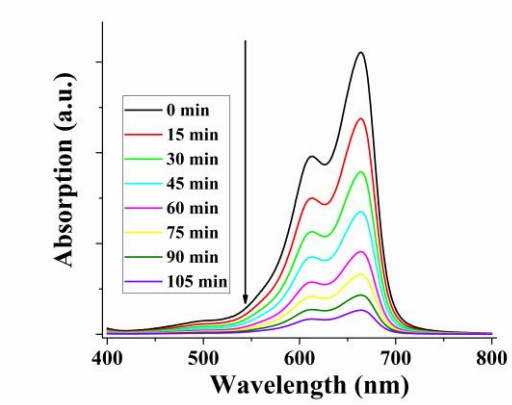

Fig. 4. UV-vis absorption spectra of MB solution using catalyst 1 in the photocatalytic experiment

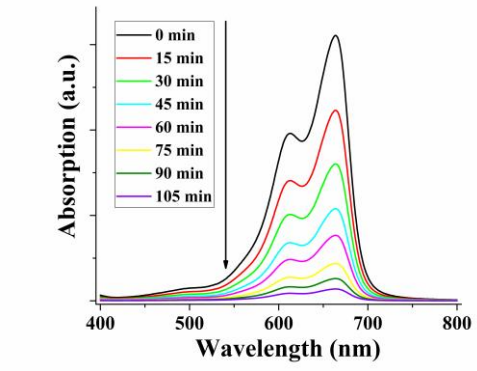

Fig. 5. UV-vis absorption spectra of MB solution using catalyst 2 in the photocatalytic experiment

In order to explore the catalytic mechanism, the catalytic experiments in the presence of scavenger benzoquinone (BQ), mannitol and ammonium oxalate (AO) were carried out (Figs. 6 and 7). The efficiencies of degradation of MB using catalysts **1** and 2 were decreased to 81.6%, 72.8%, 21.7% and 83.3%, 74.9%, 19.2%, respectively in the presence of BQ, mannitol and AO. Because BQ, mannitol and AO are $^{\bullet}O_2^-$ radical, $^{\bullet}$OH radical and the hole (h^+) scavengers, respectively, the efficiencies of degradation of MB were greatly decreased from 91.5% to 21.7% and from 95.5% to 19.2%, respectively by using catalysts **1** and **2** in the presence of scavenger AO, while they were slightly dropped in the presence of scavenger BQ and mannitol. The results exhibited that the holes (h^+) are mainly active matters for the degradation of MB, and the $^{\bullet}O_2^-$ and $^{\bullet}$OH radicals have some roles for the degradation of MB.

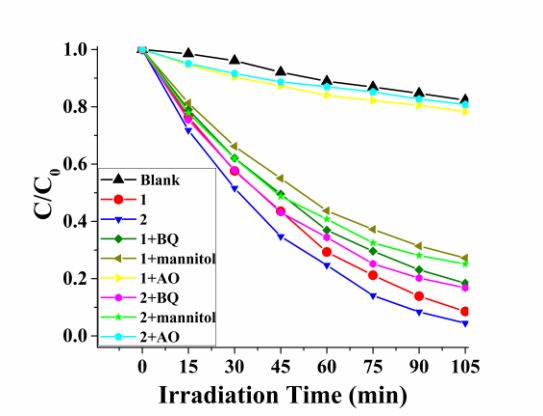

Fig. 6. Concentration changes of MB solutions in the photocatalytic experiment using catalyst 1, 2 and in the presence of scavenger BQ, mannitol and AO, and the blank experiment

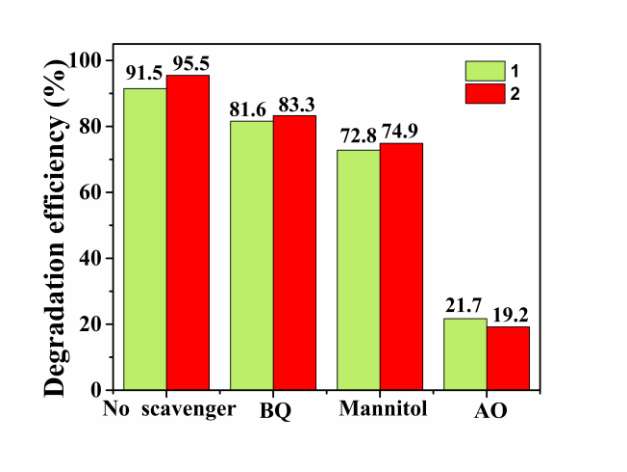

Fig. 7. Catalytic degradation efficiencies for MB using catalysts 1 and 2 in the presence of scavenger BQ, mannitol and AO, respectively

The photocatalytic mechanism of degradation of MB was proposed[9-12]. The electrons of the valence band (VB) in the photocatalysts **1** and **2** can be transferred to the conduction band (CB), leaving the holes (h^+) in the VB, when the photocatalysts were excited by the visible light with enough energy (equal to or greater than the energy band gaps: 2.453 eV for **1**, 2.162 eV for **2**). The generated electrons can interact with O_2 to generate the active species $^{\bullet}O_2^-$ radicals or interact with H_2O_2 to produce $^{\bullet}$OH radicals. The holes (h^+), $^{\bullet}$OH radicals and $^{\bullet}O_2^-$ radicals can oxidize organic dye MB to generate CO_2, H_2O or other small molecules.

4 CONCLUSION

Two copper(II) coordination polymers were successfully synthesized and characterized. **1** shows the 2*D* network with the point symbol of (4^4 6^2) and 2*D* → 2*D* polythreaded network. **2** exhibits the 6-connected 3*D* network based on the [$Cu_2(COO)_2$] dimer with the point symbol of (4^4 6^{10} 8). **1** and **2** are good photocatalysts for the degradation of methylene blue.

REFERENCES

(1) Li, W. W.; Yu, H. Q.; He, Z. Towards sustainable wastewater treatment by using microbial fuel cells-centered technologies. *Energy Environ. Sci.* **2014**, 7, 911–924.

(2) Bizani, E.; Fytianos, K.; Poulios, I. V.; Tsiridis, V. Photocatalytic decolorization and degradation of dye solutions and wastewaters in the presence of titanium dioxide. *J. Hazard. Mater*. **2006**, 136, 85–94.

(3) Dias, E. M.; Petit, C. Towards the use of metal-organic frameworks for water reuse: a review of the recent advances in the field of organic pollutants removal and degradation and the next steps in the field. *J. Mater. Chem. A* **2005**, 3, 22484–22506.

(4) Liu, G. M.; Li, X. Z.; Zhao, J. C. Photooxidation pathway of sulforhodamine-B. Dependence on the adsorption mode on TiO_2 exposed to visible light radiation. *Environ. Sci. Technol*. **2000**, 34, 3982–3990.

(5) Chen, Q.; Tong, R.; Chen, X.; Xue, Y.; Xie, Z.; Kuang, Q.; Zheng, L. Ultrafine ZnO quantum dot-modified TiO_2 composite photocatalysts: the role of the quantum size effect in heterojunction-enhanced photocatalytic hydrogen evolution. *Catal. Sci. Technol*. **2018**, 8, 1296–1303.

(6) Tang, Z. R.; Han, B.; Han, C.; Xu, Y. J. One-dimensional CdS based materials for artificial photoredox reactions. *J. Mater. Chem. A* **2017**, 5, 2387–2410.

(7) Mosleh, S.; Rahimi, M. R.; Ghaedi, M.; Dashtian, K.; Hajati, S. Sonochemical-assisted synthesis of $CuO/Cu_2O/Cu$ nanoparticles as efficient photocatalyst for simultaneous degradation of pollutant dyes in rotating packed bed reactor: LED illumination and central composite design optimization. *Ultrason. Sonochem*. **2018**, 40, 601–610.

(8) Alvaro, M.; Carbonell, E.; Ferrer, B.; Xamena, F. X. L.; Carcia, H. Semiconductor behavior of a metal-organic framework (MOF). *Chem. Eur. J*. **2007**, 13, 5106–5112.

(9) Wang, C. C.; Li, J. R.; Lv, X. L.; Zhang, Y. Q.; Guo, G. S. Photocatalytic organic pollutants degradation in metal-organic frameworks. *Energy Environ. Sci.* **2014**, 7, 2831–2867.

(10) Xu, W. T.; Ma, L.; Ke, F.; Peng, F. M.; Xu, G. S.; Shen, Y. H.; Zhu, J. F.; Qiu, L. G.; Yuan, Y. P. Metal-organic frameworks MIL-88A hexagonal microrods as a new photocatalyst for efficient decolorization of methylene blue dye. *Dalton Trans*. **2014**, 43, 3792–3798.

(11) Dong, J. P.; Shi, Z. Z.; Li, B.; Wang, L. Y. Synthesis of a novel 2*D* zinc(II) metal-organic framework for photocatalytic degradation of organic dyes in water. *Dalton Trans*. **2019**, 48, 17626–17632.

(12) Qian, L. L.; Baltov, V. A.; Wang, Z. X.; Ding, J. G.; Zhu, L. M.; Li, K.; Li, B. L.; Wu, B. Sonochemical synthesis and characterization of four nanostructural nickel coordination polymers and photocatalytic degradation of methylene blue. *Ultrason. Sonochem*. **2019**, 56, 213–218.

(13) Duan, X.; Zheng, W.; Yu, B.; Ji, Z. G. A microporous metal-organic framework with soc topology for adsorption and separation selectivity of C_2H_2/CO_2. *Chem. Pap*. **2019**, 73, 2371–2375.

(14) He, Y. P.; Tan, Y. X.; Zhang, J. Gas sorption, second-order nonlinear optics, and luminescence properties of a series of lanthanide-organic frameworks based on nanosized tris((4-carboxyl)phenylduryl)amine ligand. *Inorg. Chem*. **2013**, 52, 12758–12762.

(15) Shi, L.; Shao, D.; Shen, F. Y.; Wei, X. Q.; Wang, X. Y. A three-dimensional Mn^{II}-$[Mo^{III}(CN)_7]_4^-$ ferrimagnet containing formate as a second bridging ligand. *Chin. J. Chem*. **2019**, 38, 19–24.

(16) Pan, M.; Liao, W. M.; Yin, S. Y.; Sun, S. S.; Su, C. Y. Single-phase white-light emitting and photoluminescent color-tuning coordination assemblies. *Chem. Rev*. **2018**, 118, 8889−8935.

(17) Wang, H. P.; Wang, H. L.; Li, B. L. Synthesis, structure, luminescence and thermal stability properties of a new (3,4)-connected 2*D* Zn coordination polymer. *Chin. J. Struct. Chem*. **2020**, 39, 1835–1840.

(18) Hu, Z.; Deibert, B. J.; Li, J. Luminescent metal-organic frameworks for chemical sensing and explosive detection. *Chem. Soc. Rev*. **2014**, 43, 5815–5840.

(19) Ju, P.; Zhang, E. S.; Wang, X.; Yang, H.; Wang, J. J. A novel 3*D* Cd-based luminescence metal-organic framework: synthesis, structure and luminescent sensing properties. *Chin. J. Chem.* **2019**, 38, 1578–1584.

(20) Wang, C. K.; Xing, F. F.; Bai, Y. L.; Zhao, Y. M.; Li, M. X.; Zhu, S. R. Synthesis and structure of semirigid tetracarboxylate copper(II) porous coordination polymers and their versatile high-efficiency catalytic dye degradation in neutral aqueous solution. *Cryst. Growth Des*. **2016**, 2277–2288.

(21) Kitagawa, S.; Kitaura, R.; Noro, S. Functional porous coordination polymers. *Angew. Chem. Int. Ed*. **2004**, 43, 2334–2375.

(22) Lin, Z. J.; Lu, J.; Hong, M.; Cao, R. Metal-organic frameworks based on flexible ligands (FL-MOFs): structures and applications. *Chem. Soc. Rev*. **2014**, 43, 5867–5895.

(23) Zheng, C. Y.; Yang, H. W.; Wang, J. D.; Man, T. L.; Zhao, Z. B.; Zhao, H. K.; Wang, X. G.; Yang, E. C. A novel three-dimensional triazole-based zinc(II) coordination polymer controlled by the spacers of dicarboxylate ligand with $(4^2{\cdot}6^2{\cdot}8^2)(4{\cdot}6^2{\cdot}8^3)$ topology. *Chin. J. Struct. Chem*. **2019**, 38, 1571–1577.

(24) Xu, G. C.; Ding, Y. J.; Okamura, T.; Huang, Y. Q.; Bai, Z. S.; Hua, Q.; Liu, G. X.; Sun, W. Y.; Ueyama, N. Coordination polymers with varied metal centers and flexible tripodal ligand 1,3,5-tris(imidazol-1-ylmethyl)benzene: synthesis, structure, and reversible anion exchange property. *Cryst. Growth Des*. **2009**, 9, 395–403.

(25) Lv, X. X.; Shi, L. L.; Li, K.; Li, B. L.; Li, H. Y. An unusual porous cationic metal-organic framework based on tetranuclear hydroxyl-copper(II) cluster for fast and highly efficient dichromate trapping through a single-crystal to single-crystal process. *Chem. Commun*. **2017**, 53, 1860–1863.

(26) Qin, J. H.; Ma, L. F.; Hu, Y.; Wang, L. Y. Syntheses, structures and photoluminescence of five zinc(II) coordination polymers based on 5-methoxyisophthalate and flexible N-donor ancillary ligands. *CrystEngComm.* **2012**, 14, 2891–2898.

(27) Zheng, L. Y.; Li, K.; Zhao, S.; Liu, L.; Li, B. L.; Wu, B. Syntheses, structures and properties of eight coordination polymers based on bis(imidazole) and biscarboxylate ligands. *Polyhedron* **2016**, 104, 1–8.

(28) Sheldrick, G. M. *SHELXS-2016, Program for Crystal Structure Solution.* University of Göttingen, Germany **2016**.

(29) Sheldrick, G. M. *SHELXL-2016, Program for the Refinement of Crystal Structures from Diffraction Data.* University of Göttingen, Germany **2016**.

(30) Blatov, V. A.; Shevchenko, A. P.; Proserpio, D. M. Applied topological analysis of crystal structures with the program package ToposPro. *Cryst. Growth Des*. **2014**, 14, 3576–3586.